Journal of Magnetism and Magnetic Materials 370 (2014) 81–86

Contents lists available at ScienceDirect

Journal of Magnetism and Magnetic Materials

journal homepage: www.elsevier.com/locate/jmmm

Tuning Fermi level of Cr_2CoZ (Z=Al and Si) inverse Heusler alloys via Fe-doping for maximum spin polarization

Mukhtiyar Singh [a], Hardev S. Saini [b], Jyoti Thakur [a], Ali H. Reshak [c,d], Manish K. Kashyap [a,*]

[a] Department of Physics, Kurukshetra University, Kurukshetra-136119, Haryana, India
[b] Department of Physics, Panjab University, Chandigarh-160014, India
[c] New Technologies—Research Center, University of West Bohemia, Univerzitni 8, 306 14 Pilsen, Czech Republic
[d] Center of Excellence Geopolymer and Green Technology, School of Material Engineering, University Malaysia Perlis, 01007 Kangar, Perlis, Malaysia

ARTICLE INFO

Article history:
Received 22 October 2013
Received in revised form
13 June 2014
Available online 24 June 2014

Keywords:
Heusler alloys
DFT
Half-metallic ferromagnetism

ABSTRACT

We report full potential treatment of electronic and magnetic properties of $Cr_{2-x}Fe_xCoZ$ (Z=Al, Si) Heusler alloys where $x=0.0$, 0.25, 0.5, 0.75 and 1.0, based on density functional theory (DFT). Both parent alloys (Cr_2CoAl and Cr_2CoSi) are not half-metallic frromagnets. The gradual replacement of one Cr sublattice with Fe induces the half-metallicity in these systems, resulting maximum spin polarization. The half-metallicity starts to appear in $Cr_{2-x}Fe_xCoAl$ and $Cr_{2-x}Fe_xCoSi$ with $x=0.50$ and $x=0.25$, respectively, and the values of minority-spin gap and half-metallic gap or spin-flip gap increase with further increase of x. These gaps are found to be maximum for $x=1.0$ for both cases. An excellent agreement between the structural properties of CoFeCrAl with available experimental study is obtained. The Fermi level tuning by Fe-doping makes these alloys highly spin polarized and thus these can be used as promising candidates for spin valves and magnetic tunnelling junction applications.

1. Introduction

Heusler alloys represent a class of materials which show a number of diverse magnetic phenomena [1,2]. Many of these alloys have conducting nature for one spin channel and semiconducting for the other. The Heusler alloys with this type of character are known as Half-metalllic ferromagnets (HMFs). The half-metallic (HM) Heusler alloys generally display high Curie temperatures, but more importantly they are in certain cases closely lattice-matched to semiconductors. For example, Co_2FeSi is ferromagnetic up to temperatures 1000 K and is lattice-matched to GaAs within ~0.08% [3–6]. Since the prediction of HM nature of NiMnSb Heusler alloy [7], a significant scientific thrust has been observed towards the HM Heusler alloys. Apart from various theoretical studies on these alloys and other HM materials [8–14], the HM character have also been very well confirmed experimentally [15–17]. These alloys, due to the 100% spin polarized current, are expected to improve significantly the performance of magnetic tunnelling junctions (MTJs) based on the tunnelling magnetoresistance (TMR) [18].

The conventional ternary Heusler alloys with stoichiometric composition, X_2YZ and XYZ, exist in $L2_1$ and $C1_b$ crystal structures, respectively, with X and Y as the two transition metal (TM) atoms and Z as a main group element. If one of the X atoms in X_2YZ structure is replaced by a IIIrd TM atom (X′), the resulting alloy gets crystallized in the Y-structure, XX′YZ (Prototype LiMgPdSn), which has no inversion symmetry. These are classified as quaternary Heusler alloys. These 1:1:1:1 quaternary Heusler alloys can be converted back to the ternary structure by replacing the X atom with the Y atom. The consequential structure (X′Y_2Z) so formed is known as the X-structure (prototype $CuHg_2Ti$). This structure often appears for Heusler alloys when the X′ element is more valent than that of the Y and both elements are from the same, 3d TM, period. The Heusler alloys with this structure are often named as inverse Heusler alloys. These alloys are known for their small magnetic moment and high Curie temperature [19] due to strong direct exchange interaction between like atoms. Various theoretical and experimental studies have been devoted to these systems [20–23].

The large TMR ratio, which is determined by the spin polarization of ferromagnetic electrodes, can be obtained by using the electrodes of Heusler alloys in MTJs. Sakuraba et al. [24] verified this fact in Co_2MnSi/Al–O/Co_2MnSi MTJ by showing a high value (570%) of TMR in this system. The current perpendicular to plane–giant magnetoresistance (CPP–GMR) ratio can also be enhanced by using highly spin polarized Heusler alloys as ferromagnetic electrodes [25]. However, the spin polarization of these materials greatly influenced by temperature, spin wave excitation and the narrow energy separation between the Fermi level (E_F) and the conduction or valence band edge [26] which ultimately hinder their practical applications. This problem might be solved by

* Corresponding author.
E-mail addresses: manishdft@gmail.com, mkumar@kuk.ac.in (M.K. Kashyap).

http://dx.doi.org/10.1016/j.jmmm.2014.06.050
0304-8853/

choosing a Heusler alloy with E_F lying almost at the center of a large minority-spin gap ($E_{g\downarrow}$) or shifting the E_F in to mid of this gap by doping with another suitable TM element.

It is established that E_F tuning would be one of the essential techniques to achieve the materials with higher spin polarization [13]. This tuning can be achieved by suitable doping in stoichiometric Heusler alloys. Tezuka et al. [27] demonstrated the E_F tuning in Co-based full Heusler alloys by substituting Z with an element of a different valence and obtained a larger value of effective spin polarization, in $Co_2FeAl_{0.5}Si_{0.5}$, as compared to the stoichiometric composition i.e. Co_2FeSi or Co_2MnAl. Inomata et al. [28] demonstrated large TMR, 16% at room temperature and 26.5 at% 5 K, in Fe doped $Co_2Cr_{0.6}Fe_{0.4}Al$ Heusler alloy film. The enhancement of spin polarization was also confirmed using Fe doping in Co_2MnSn by employing Andreev Reflection technique [29]. We have been motivated by this point and demonstrated in the present work how position of E_F can be pinned in middle of $E_{g\downarrow}$ via doping of Fe for Cr in Cr_2CoZ (Z=Al, Si) inverse Heusler alloys to get the maximum degree of spin polarization.

2. Computational details

The electronic structure calculations of stoichiometric and off-stoichiometric $Cr_{2-x}Fe_xCoZ$ (Z=Al and Si) Heusler alloys where x=0.0, 0.25, 0.50, 0.75 and 1.0, were carried out using the DFT [30] based full potential linear augmented plane wave (FPLAPW) method as implemented in WIEN2k [31]. In FPLAPW calculations, the core states were treated fully relativistically, whereas, for the valence states a scalar relativistic approximation was used. The exchange and correlation (XC) potentials were constructed using generalized gradient approximation (GGA) within the parameterization of Perdew–Burke–Ernzerhof [32]. Additionally, the valence electron wave function inside the muffin-tin (MT) sphere was expanded up to l_{max}=10. The Radii of MT sphere (R_{MT}) for various atoms were taken in the present calculations such as to ensure the nearly touching spheres. The plane wave cut-off parameters were decided by $R_{MT}k_{max}$=7 (where k_{max} is the largest wave vector of the basis set such that k_{max} controls the accuracy of the calculation) and G_{max}=12 a.u.$^{-1}$ for Fourier expansion of potential in the interstitial region. A conventional $1\times1\times1$ cell of 16 atoms was generated to simulate the various doping concentrations. The k-space integration was carried out using the modified tetrahedron method [33]. A $17\times17\times17$ k-point mesh was used as base for this integration resulting in 455/63 k-points for stoichiometric/off-stoichiometric alloys in the irreducible Brillouin zone. The energy convergence criterion was set to 10^{-4} Ry/cell and the charge convergence was also monitored along with it. Further, full relaxations of the internal atomic coordinates have also been carried out prior to studying the electronic and magnetic properties of the present systems.

The Cr_2CoZ (Z=Al and Si) inverse Heusler alloys crystallizes in X-structure and the Wyckoff positions for this structure are 4a (0, 0, 0), 4b (1/2, 1/2, 1/2), 4c (1/4, 1/4, 1/4) and 4d (3/4, 3/4, 3/4), where Cr occupies the two inequivalent 4a and 4c sites as nearest neighbors. In our nomenclature, they are represented by Cr^{I} and Cr^{II} and we use this terminology throughout the text. Beside this, Co and Z atoms reside at 4b and 4d, respectively.

3. Result and discussion

The results have been described in two parts. In first part, only stoichiometric Cr_2CoZ (Z=Al and Si) inverse Heusler alloys without doping have been considered whereas in second part, the Fe-doping in these alloys has been taken in to account.

3.1. Stoichiometric Cr_2CoZ (Z=Al and Si) inverse Heusler alloys

The parent Cr_2CoZ (Z=Al and Si) inverse Heusler alloys are recently proposed by Skaftouros et al. [34]. Both alloys energetically favour X-structure which has been confirmed in this work using Murnaghan equation of state [35]. Fig. 1 shows the optimization plots for Cr_2CoSi in $L2_1$ and X-structure as a representative. Here, X-structure is found to be more stable than the corresponding $L2_1$-structure by an energy $E\sim1.0$ eV. The obtained lattice parameters, shown in Table 1, are in very good agreement with the previously calculated values [34].

The total DOS of both alloys are almost similar. Fig. 2 (upper panel) shows the calculated DOS of Cr_2CoZ (Z=Al and Si) alloys. It clearly manifests the strong metallic character of the majority-spin channel (MAC). The presence of finite DOS at E_F in minority-spin channel (MIC) separates them from the HMF category. These alloys do not have a gap in MIC, however, the calculated values of spin polarization, $P=[n_\uparrow(E_F)-n_\downarrow(E_F)]/[n_\uparrow(E_F)+n_\downarrow(E_F)]$ are still appreciable i.e. 68% and 94% for Cr_2CoAl and Cr_2CoSi, respectively.

In order to have better insight of the electronic structure, we have taken Cr_2CoSi as representative and explained the necessary ingredients of the DOS (lower panel of Fig. 2). In MAC, a three peaks structure is identified. The two are in bonding region whose origin is e_g-t_{2g} splitting of d-states of Cr^{I} and Co atoms in the cubic crystal field [36]. The third one in antibonding region is mainly of Cr^{I} nature. The d-states of Cr^{II} atom present in a localized manner at E_F. In MIC, similar peaks exist in bonding region. The d-states of Cr^{II} states which are localized at E_F in MAC get blue shifted by $\sim$1.0 eV relative to E_F due to large exchange splitting of Cr atoms. It is clear from the behaviour of DOS that the covalent hybridization between lower-energy Cr-d states and higher-energy Co-d states is responsible for the formation of bonding and antibonding states [9]. The p-states of Si-atoms which lie deep from ~-6.0 to -2.0 eV (not shown for brevity), do not take part in the formation of gap in MIC, nevertheless, they effectively determine the occupancy of p–d orbitals and decide the position of E_F after hybridization with TM-d states.

The Cr_2CoZ (Z=Al and Si) Heusler alloys are actually HM ferrimagnets [34] due to antiferrornagnetic coupling between two inequivalent nearest neighbours Cr-atoms. Out of two alloys, Cr_2CoAl is fully compensated ferrimagnet (FCF) [37] with exactly 24 valence electrons. According to Slater-Pauling rule,

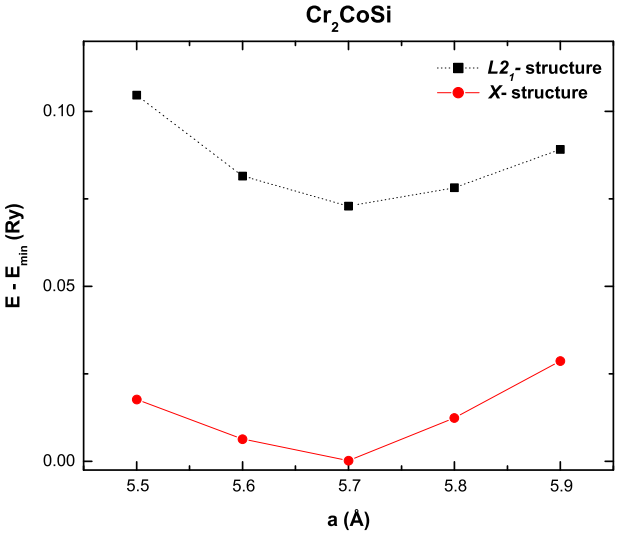

Fig. 1. Calculated total energy vs. the lattice parameter of Cr_2CoSi in the $L2_1$ and X-structure. The zero of the energy corresponds to the global equilibrium lattice constant.

Table 1
The calculated lattice parameters, total and atom-resolved spin magnetic moment (in μ_B) along with spin polarization (P) of $Cr_{2-x}Fe_xCoZ$ (Z=Al, Si; x=0.0, 0.25, 0.5, 0.75 and 1.0) inverse Heusler alloys.

Compound		a (Å)	m_{tot}	m_{Fe}	m^{I}_{Cr}	m^{II}_{Cr}	m_{Co}	m_Z	P
Cr_2CoAl	This work	5.77	0.00	–	−1.45	1.25	0.27	−0.02	0.68
	Other	5.80[a]	0.01	–	−2.10	1.87	0.30	−0.05[a]	–
$Cr_{1.75}Fe_{0.25}CoAl$	This work	5.75	0.37	0.49	−1.48	1.28	0.39	−0.04	0.97
	Other	–	–	–	–	–	–	–	–
$Cr_{1.50}Fe_{0.50}CoAl$	This work	5.72	0.80	0.25	−1.53	1.30	0.46	−0.05	0.99
	Other	–	–	–	–	–	–	–	–
$Cr_{1.25}Fe_{0.75}CoAl$	This work	5.71	1.04	0.23	−1.61	1.35	0.71	−0.04	0.99
	Other	–	–	–	–	–	–	–	–
CoFeCrAl	This work	5.70	2.00	0.60	–	1.60	1.03	−0.04	1.00
	Other	5.71[b]	2.00[b]	–	–	–	–	–	–
	Expt	5.73[c]	–	–	–	–	–	–	–
Cr_2CoSi	This work	5.67	1.00	–	−0.76	1.15	0.69	−0.03	0.94
	Other	5.67[a]	1.06	–	−1.11	1.61	0.54	−0.04[a]	–
$Cr_{1.75}Fe_{0.25}CoSi$	This work	5.65	2.22	0.43	−0.94	1.43	0.72	−0.03	0.99
	Other	–	–	–	–	–	–	–	–
$Cr_{1.50}Fe_{0.50}CoSi$	This work	5.64	2.63	0.45	−0.97	1.45	0.86	−0.03	0.99
	Other	–	–	–	–	–	–	–	–
$Cr_{1.25}Fe_{0.75}CoSi$	This work	5.62	2.80	0.45	−0.99	1.50	1.00	−0.04	1.00
	Other	–	–	–	–	–	–	–	–
CoFeCrSi	This work	5.61	3.00	0.32	–	1.64	1.06	−0.04	1.00
	Other	5.63[b]	3.00[b]	–	–	–	–	–	–

[a] Ref. [34].
[b] Ref. [40].
[c] Ref. [41].

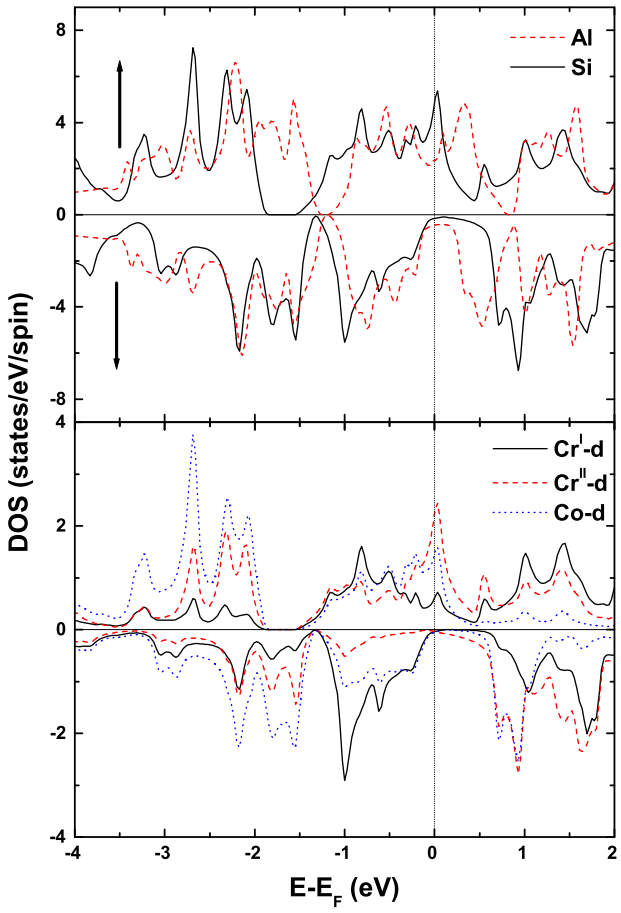

Fig. 2. Total DOS (upper panel) of stoichiometric Cr_2CoZ (Z=Al, Si) inverse Heusler alloys and partial DOS (lower panel) of Cr_2CoSi inverse Heusler alloys. E_F corresponds to Fermi level (E_F).

$m_t = N_V - 24$, the total spin magnetic moment for FCF should be exactly zero. The calculated total and atom resolved spin magnetic moments are listed in Table 1. The calculated total spin magnetic moments are in accordance with Slater-Pauling rule for both Cr_2CoZ (Z=Al and Si). Co carries local spin magnetic moment of 0.27 μ_B for Cr_2CoAl and 0.69 μ_B for Cr_2CoSi. Z-atoms carry a negligibly small induced moment aligned antiparallel with Co. In both alloys, Cr-atoms carry magnetic moments with opposite polarity due to their mutual antiparallel alignment. It can be explained in the following way: In Heusler alloys, there are primarily two magnetic processes, i.e. exchange splitting of d-states of magnetic atoms and the interatomic covalent interaction of d-states [38]. The former equally favours both alignments i.e. ferromagnetic and antiferromagnetic, whilst only antiferromagnetic alignment dominates due to latter [39]. More precisely, it is a competition between these two processes which decides the ferromagnetic or antiferromagnetic alignment of atomic magnetic moments in these alloys. The strong direct interaction between d-states of nearest neighboured inequivalent Cr-atoms makes them to align antiparallel with each other. Due to this, almost vanishing total spin magnetic moment appears in Cr_2CoAl FCF and a small value for Cr_2CoSi ferrimagnet.

3.2. Doped $Cr_{2-x}Fe_xCoZ$ (Al and Si) Heusler alloys

As discussed in introduction, the position of E_F in the minority band gap determines the quality of the half-metallicity. To have the large HM gap or spin-flip gap, E_{sf}, (energy for transition from half-metal to traditional ferromagnet/ferrimagnet), which would be the most desirable in half-metals for spintronics utility, the E_F must lie almost in the middle of the $E_{g\downarrow}$. The modification of electronic structure and physical properties of Cr_2CoZ (Z=Al, Si) Heusler alloys were carried out by doping with a fourth TM i.e. Fe which can provide a class of materials with tailored characteristics. Fig. 3 shows the variation of lattice parameters (a) of resultant alloys as a function of doping concentration x. The lattice

parameters of $Cr_{2-x}Fe_xCoZ$ (Z=Al and Si) decrease linearly with the increase in x. The optimized lattice parameters are summarized in Table 1.

Fig. 4 shows the calculated total DOS of doped $Cr_{2-x}Fe_xCoZ$ (Al and Si) Heusler alloys for x=0.0, 0.25, 0.50, 0.75 and 1.0. As for the stoichiometric alloys, discussed above, the MAC holds the metallic character throughout for all doping concentrations here also. The DOS in MIC, on the other hand, changes its nature continuously with the Fe substitution. The gradual replacement of one of the Cr sublattices with Fe splits the DOS at E_F in MIC. This splitting increase as we increase Fe-doping and complete replacement of one of the Cr sublattice with Fe creates a new quaternary Heusler alloy, CoFeCrZ (Z=Al and Si) which crystallize in Y-structure. This study endorses by the previous study on CoFeCrZ (Al and Si) quaternary Heusler alloys [40]. Further, the calculated lattice constant (Table 1) and site occupation of various atoms in CoFeCrAl alloy are also in accordance with the recent experiment study by Nehra et al. [41] on this compound. This verifies the credibility of this work.

The variation of $E_{g\downarrow}$ and E_{sf} with Fe concentration (x) is presented in Fig. 5. After the onset of half metallicity, with x=0.50 and x=0.25, respectively, in $Cr_{2-x}Fe_xCoAl$ and $Cr_{2-x}Fe_xCoSi$, there is increase in both energy gaps, $E_{g\downarrow}$ and E_{sf}, with higher value of x. The maximum value of $E_{g\downarrow}$ and E_{sf} are found to be 0.485/0.672 and 0.156/0.320 eV, respectively, for x=1 in $Cr_{2-x}Fe_xCoAl$/$Cr_{2-x}Fe_xCoSi$. The almost 100% spin-polarization which initialize with x=0.50 and x=0.25, respectively, in $Cr_{2-x}Fe_xCoAl$ and $Cr_{2-x}Fe_xCoSi$ and remain almost saturated at maximum (100%)

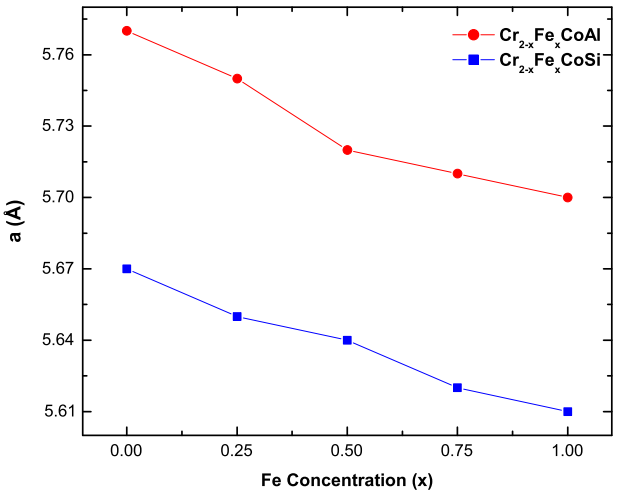

Fig. 3. The variation of lattice parameters (a) with Fe-concentration (x) in $Cr_{2-x}Fe_xCoZ$ (Z=Al, Si; x=0.0, 0.25, 0.5, 0.75 and 1.0) Heusler alloys.

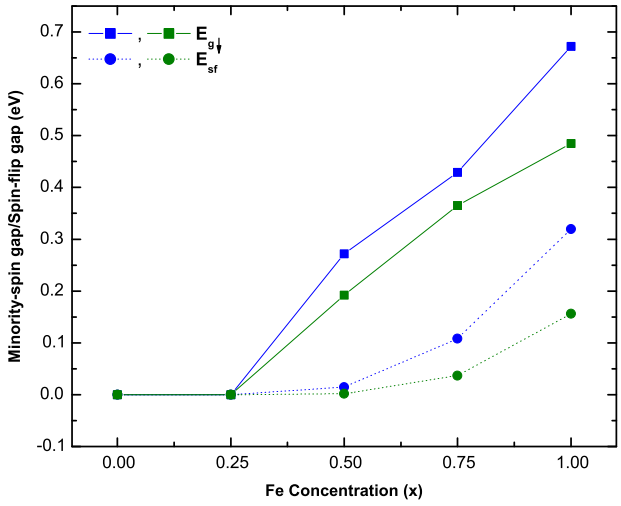

Fig. 5. Minority-spin gap ($E_{g\downarrow}$) and HM gap or spin-flip gap (E_{sf}) as a function of Fe-concentration (x). The sphere with solid line/dotted line (olive color) represents $E_{g\downarrow}$/E_{sf} for $Cr_{2-x}Fe_xCoAl$ and the square with solid line/dotted line (blue color) represents $E_{g\downarrow}$/E_{sf} for $Cr_{2-x}Fe_xCoSi$ where x=0.0, 0.25, 0.5, 0.75 and 1.0. (For interpretation of the references to color in this figure legend, the reader is referred to the web version of this article.)

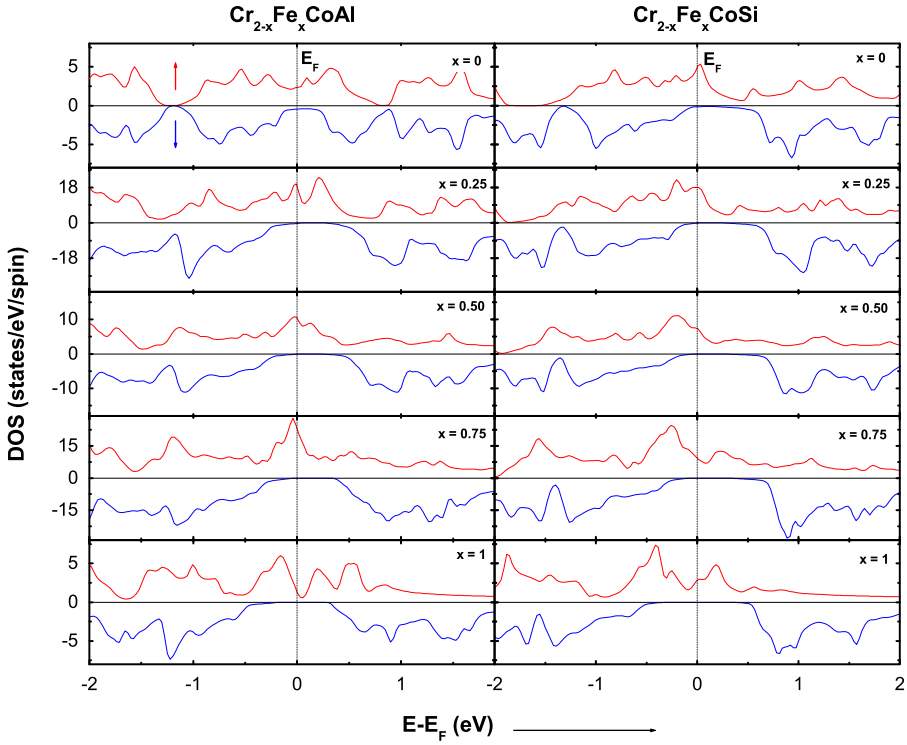

Fig. 4. Total DOS of undoped and Fe-doped Cr_2CoZ (Z=Al, Si) inverse Heusler alloys at Fe-concentrations, x=0.0, 0.25, 0.5, 0.75 and 1.0.

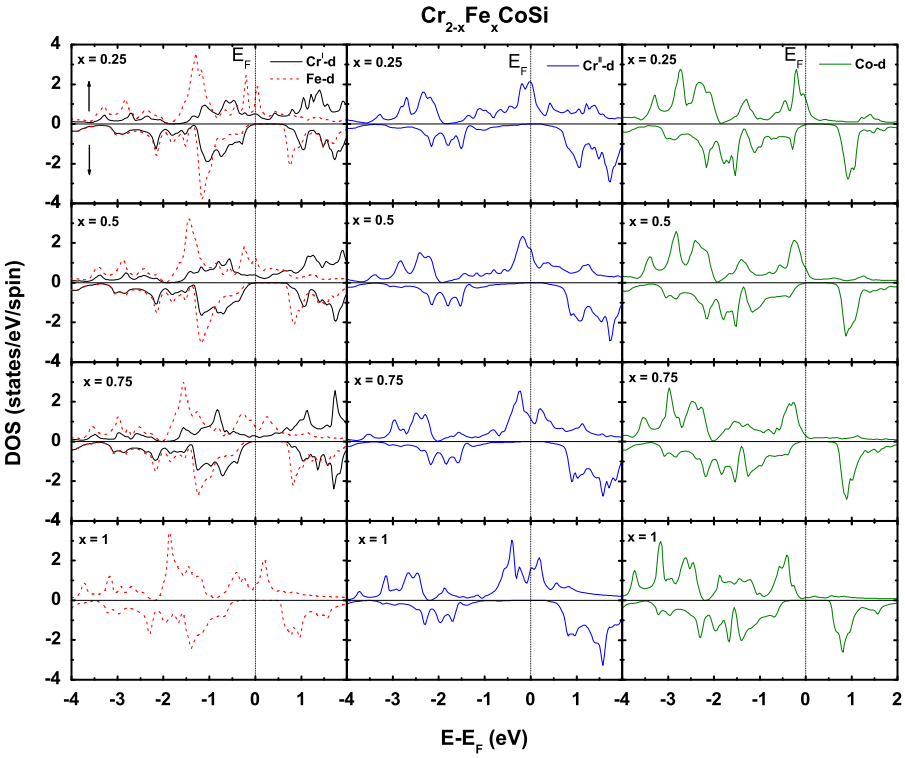

Fig. 6. Atom resolved d-DOS of $Cr_{2-x}Fe_xCoSi$ (x=0.25, 0.5, 0.75 and 1.0) Heusler alloys.

for further increase in x for both alloys (Table 1). The increment in spin polarization with the Fe-doping in $Cr_{2-x}Fe_xCoSi$, for example, may be due to behaviour of Fe as electron dopant for this substitution. Thus, the number of extra electrons is to be adjusted only in the MAC if the alloys have to follow the Slater-Pauling rule [9,29]. This leads to the appearance of small DOS in MAC in the vicinity of E_F. This is illustrated in Fig. 6 (left panel). For x=1.0, Fe completely replaces the one Cr sublattice and interaction between the TM atoms gets modified and E_F falls exactly in the middle of minority band gap. The strong hybridization between TM atoms and further with sp atoms might be the reason for the shifting of E_F.

When we move from x=0.0 to x=1.0, the two extra electrons are added up and the number of valence electrons increases from 24 to 26 in CoFeCrAl and from 25 to 27 in CoFeCrSi. This leads to the increase of total spin magnetic moments from 0.00 μ_B to 2.00 μ_B and 1.00 μ_B to 3.00 μ_B in $Cr_{2-x}Fe_xCoAl$ and $Cr_{2-x}Fe_xCoSi$ (for x=1.0), respectively. As discussed in Section 3.1, for the stoichiometric composition, 3d states of TM atoms form the common d-band; hence localized partial magnetic moments composed of itinerant electrons are obtained [39]. The d-DOS of $Cr_{2-x}Fe_xCoSi$ (x=0.25, 0.50, 0.75 and 1.0), in Fig. 6, clearly indicates the localized behaviour of magnetic moment in these alloys.

The calculated total spin magnetic moments (Table 1) increase as x varies from 0.0 to 1.0. The Cr^{II} atom carries the major part of the total moment and this moment gets enhanced with increase of Fe-doping. Further, the moment at Co site also shows a linear increase with incremental Fe substitution. Fe also carries a small moment for all concentrations in both systems and its ferromagnetic alignment with Cr^{II} atom possibly leads to the enhancement of total spin magnetic moment of the resulting alloys. Z-atoms have a negligibly small magnetic moment, similar to the stoichiometric case, which aligns in antiparallel configuration. The magnetic properties of 3d-metals solely depend on the chemical environment surrounding them. As substitution of Cr^{I} with Fe changes the chemical environment and the reconstruction of the 3d bands takes place which leads to change in the magnetic moments.

4. Summary and conclusions

First-principles calculations based on DFT for undoped and Fe-doped Cr_2CoZ (Z=Al, Si) inverse Heusler alloys have been performed in order to search half-metallicity. Both parent (undoped) alloys: Cr_2CoAl and Cr_2CoSi are not found to be true HMFs. On the other hand, the half-metallicity starts to appear in these systems with Fe-doping and spin polarization (P) raises with increase in doping concentration of Fe (x). The half-metallicity starts to appear in $Cr_{2-x}Fe_xCoAl$ and $Cr_{2-x}Fe_xCoSi$ with x=0.50 and x=0.25, respectively. The spin polarization remains almost saturated at 100% for higher value of x in both alloys. The end alloys i.e. x=1, carries the maximum value of minority-spin gap and spin-flip gap which are found to be 0.672 and 0.320 eV, respectively, for $Cr_{2-x}Fe_xCoAl$ and $Cr_{2-x}Fe_xCoSi$. A very good agreement has been found for the structural properties of CoFeCrAl with available experimental study which justifies the authenticity of this work. The alteration of electronic properties of $Cr_{2-x}Fe_xCoZ$ (Z=Al, Si) Heusler alloys in a desired way via tuning of E_F would be proved as essential technique to achieve the materials with higher spin polarization and proposed systems may be used as the ideal candidate for spin valves and MTJ applications. We hope that the present work will encourage further experimental studies of HM systems based on these Heusler alloys and promote more studies on the same.

Acknowledgements

The work is supported by UGC, INDIA grant no. 41-922/2012 (SR). M. Singh acknowledges UGC for providing financial assistantship in form of SRF-RGNFS. For the author A.H. Reshak, the results

were developed within the CENTEM project, Reg. no. CZ.1.05/2.1.00/03.0088, co-funded by the ERDF as part of the Ministry of Education, Youth and Sports OP RDI program "MetaCentrum and the CERIT-SC under the program Center CERIT Scientific Cloud reg. no.CZ.1.05/3.2.00/08.0144".

References

[1] P.J. Webster, K.R.A. Ziebeck, in: H.R.J. Wijn (Ed.), Alloys and Compounds of d-Elements with Main Group Elements. Part 2, Landolt-Bornstein, New Series, Group III, 19, Springer, Berlin, 1986, pp. 75–184;
C.T. Tanaka, J. Nowak, J.S. Moodera, J. Appl. Phys. 86 (1999) 6239.
[2] K.R.A. Ziebeck, K.U. Neumann, Magnetic Properties of Metals, Landolt-Börnstein, New Series, Group III, 32/c, in: H.R.J. Wijn (Ed.), Springer, Berlin, 2001, pp. 64–414.
[3] R. Farshchi, M. Ramsteiner, J. Appl. Phys. 113 (2013) 191101.
[4] M. Hashimoto, J. Herfort, H.-P. Sch€onherr, K.H. Ploog, Appl. Phys. Lett. 87 (2005) 102506.
[5] M. Hashimoto, A. Trampert, J. Herfort, K.H. Ploog, J. Vac. Sci. Technol., B 25 (2007) 1453.
[6] M. Hashimoto, J. Herfort, A. Trampert, H.-P. Sch€onherr, K.H. Ploog, J. Phys. D: Appl. Phys. 40 (2007) 1631.
[7] R.A. de Groot, F.M. Mueller, P.G. van Engen, K.H.J. Buschow, Phys. Rev. Lett. 50 (1983) 2024.
[8] I. Galanakis, P.H. Dederichs, N. Papanikolaou, Phys. Rev. B: Condens. Matter 66 (2002) 134428.
[9] I. Galanakis, P.H. Dederichs, Phys. Rev. B: Condens. Matter 66 (2002) 174429.
[10] M. Kumar, T. Nautiyal, S. Auluck, J. Phys. Condens. Matter 21 (2009) 196003 (ibid 21 (2009) 446001).
[11] M. Singh, H.S. Saini, S. Kumar, M.K. Kashyap, Comput. Mater. Sci. 53 (2012) 431;
M. Singh, J. Thakur, H.S. Saini, A.H. Reshak, M.K. Kashyap, J. Alloys Compd. 580 (2013) 201.
[12] P.J. Brown, K.U. Neumann, P.J. Webster, K.R.A. Ziebeck, J. Phys. Condens. Matter 12 (2000) 1827;
P.J. Brown, A.P. Gandy, R. Kainuma, T. Kanomata, T. Miyamoto, M. Nagasako, K. U. Neumann, A. Sheikh, K.R.A. Ziebeck, J. Phys. Condens. Matter 22 (2010) 206004.
[13] H.S. Saini, M. Singh, A.H. Reshak, M.K. Kashyap, Comput. Mater. Sci. 74 (2013) 114 (J. Magn. Magn. Mater. 331 (2013) 1; J. Alloys Compds 536 (2012) 214.).
[14] J.-H. Park, E. Vescovo, H.-J. Kim, C. Kwon, R. Ramesh, T. Venkatesan, Nature 392 (1998) 794.
[15] R. Shan, H. Sukegawa, W.H. Wang, M. Kodzuka, T. Furubayashi, T. Ohkubo, S. Mitani, K. Inomata, K. Hono, Phys. Rev. Lett. 102 (2009) 246601.
[16] K.E.H.M. Hanssen, P.E. Mijnarends, L.P.L.M. Rabou, K.H.J. Buschow, Phys. Rev. B: Condens. Matter 42 (1990) 1533.
[17] Y. Sakuraba, J. Nakata, M. Oogane, H. Kubota, Y. Ando, A. Sakuma, T. Miyazaki, Jpn. J. Appl. Phys. 44 (2005) L1100.
[18] B. Balke, S. Wurmehl, G.H. Fecher, C. Felser, J. Kübler, Sci. Technol. Adv. Mater. 9 (2008) 014102.
[19] M. Meinert, J.-M. Schmalhorst, G. Reiss, J. Phys. Condens. Matter 23 (2011) 116005.
[20] I. Galanakis, K. Ozdogan, E. Sasioglu, B. Aktas, Phys. Rev. B: Condens. Matter 75 (2007) 172405.
[21] H.Z. Luo, H.W. Zhang, Z.Y. Zhu, L. Ma, S.F. Xu, G.H. Wu, X.X. Zhu, C.B. Jiang, H. B. Xu, J. Appl. Phys. 103 (2008) 083908.
[22] I. Galanakis, E. Şaşıoğlu, Appl. Phys. Lett. 99 (2011) 052509.
[23] M. Meinert, J.-M. Schmalhorst, C. Klewe, G. Reiss, E. Arenholz, T. Böhnert, K. Nielsch, Phys. Rev. B: Condens. Matter 84 (2011) 132405.
[24] Y. Sakuraba, M. Hattori, M. Oogane, Y. Ando, H. Kato, A. Sakuma, T. Miyazaki, H. Kubota, Appl. Phys. Lett. 88 (2006) 192508.
[25] K. Yakushiji, K. Saito, S. Mitani, K. Takanashi, Y.K. Takahashi, K. Hono, Appl. Phys. Lett. 88 (2006) 222504.
[26] J.J. Attema, G.A. de Wijs, R.A. de Groot, J. Phys. Condens. Matter 19 (2007) 315212.
[27] N. Tezuka, N. Ikeda, A. Miyazaki, S. Sugimoto, M. Kikuchi, K. Inomata, Appl. Phys. Lett. 89 (2006) 112514.
[28] K. Inomata, S. Okamura, R. Goto, N. Tezuka, Jpn. J. Appl. Phys. 42 (2003) L419.
[29] A. Rajanikanth, Y.K. Takahashi, K. Hono, J. Appl. Phys. 103 (2008) 103904.
[30] M. Weinert, E. Wimmer, A.J. Freeman, Phys. Rev. B: Condens. Matter 26 (1982) 4571.
[31] P. Blaha, K. Schwarz, G.K.H. Madsen, D. Kvasnicka, J. Luitz, WIEN2k, An Augmented Plane Wave+Local Orbitals Program for Calculating Crystal Properties, Karlheinz Schwarz, Techn. Universitat Wien, Wien, Austria, ISBN 3-9501031-1-2, 2001.
[32] P. Perdew, S. Burke, M. Ernzerhof, Phys. Rev. Lett. 77 (1996) 3865.
[33] P.E. Blöchl, O. Jepsen, O.K. Andersen, Phys. Rev. B: Condens. Matter 49 (1994) 16223.
[34] S. Skaftouros, K. Özdoğan, E. Şaşıoğlu, I. Galanakis, Phys. Rev. B: Condens. Matter 87 (2013) 024420.
[35] F.D. Murnaghan, Proc. Nat. Acad. Sci. U.S.A. 30 (1944) 244.
[36] G.D. Liu, X.F. Dai, H.Y. Liu, J.L. Chen, Y.X. Li, Gang Xiao, G.H. Wu, Phys. Rev. B: Condens. Matter 77 (2008) 014424.
[37] H. van Leuken, R.A. de Groot, Phys. Rev. Lett. 74 (1995) 1171.
[38] A.R. Williams, R. Zeller, V.L. Moruzzi, C.D. Gellat, J. Kubler, J. Appl. Phys. 52 (1981) 2067.
[39] J. Kübler, A.R. William, C.B. Sommers, Phys. Rev. B: Condens. Matter 28 (1983) 1745.
[40] G.Y. Gao, L. Hu, K.L. Yao, B. Luo, N. Liu, J. Alloys Compd. 551 (2013) 539.
[41] J. Nehra, V.D. Sudheesh, N. Lakshmi, K. Venugopalan, Phys. Status Solidi RRL **7** (2013) 289.